Published in final edited form as:
J Neurol. 2013 January ; 260(1): 242–252. doi:10.1007/s00415-012-6626-z.

Diffuse axonal injury in mild traumatic brain injury: a 3D multivoxel proton MR spectroscopy study

Ivan I. Kirov, PhD, **Assaf Tal, PhD**, **James S. Babb, PhD**, **Yvonne W. Lui, MD**, **Robert I. Grossman, MD**, and **Oded Gonen, PhD**
Department of Radiology, New York University School of Medicine, New York, NY, USA

Abstract

Since mild traumatic brain injury (mTBI) often leads to neurological symptoms even without clinical MRI findings, our goal was to test whether diffuse axonal injury is quantifiable with multivoxel proton MR spectroscopic imaging (^{1}H-MRSI). T1- and T2-weighted MRI and three dimensional ^{1}H-MRSI (480 voxels over 360 cm^3, ~30% of the brain) were acquired at 3 Tesla from 26 mTBI patients (mean Glasgow Coma Scale score 14.7), 18–56 years old, 3–55 days post injury and 13 healthy matched contemporaries. The *N*-acetylaspartate (NAA), choline (Cho), creatine (Cr) and *myo*-inositol (*m*I) concentrations and gray-, white-matter (GM/WM) and cerebrospinal fluid fractions were obtained in each voxel. Global GM and WM absolute metabolic concentrations were estimated using linear regression, and patients were compared with controls using two-way analysis of variance. Patients' mean NAA, Cr, Cho and *m*I concentrations in GM (8.4±0.7, 6.9±0.6, 1.3±0.2, 5.5±0.6 mM) and Cr, Cho and *m*I in WM (4.8±0.5, 1.4±0.2, 4.6±0.7 mM) were not different from controls'. NAA, however, was significantly lower in patients' than controls' WM (7.2±0.8 versus 7.7±0.6 mM, p=0.0125). The Cho and Cr levels in patients' WM positively correlated with time from mTBI. This ^{1}H-MRSI approach allowed us to ascertain that early mTBI sequelae are (*i*) diffuse (not merely local), (*ii*) neuronal (not glial) and (*iii*) in the global white (not gray) matter. These findings support the hypothesis that, similarly to more severe head trauma, mTBI also results in diffuse axonal injury, but that dysfunction, rather than cell death, dominates shortly after injury.

Keywords

Brain Injury; Diffuse Axonal Injury; Magnetic Resonance Spectroscopy

Introduction

Traumatic brain injury (TBI) annually accounts for 1.6 million emergency room visits and hospitalizations in the US [1]. It is suspected that many more victims do not seek medical attention or are seen at their doctor's office. Patients who do not recover add to the 1% of the US population living with TBI-related, long-term disability [2]. Moreover, TBI from blast exposure has been described as the “signature injury” of the recent wars in Iraq and Afghanistan [3] with ~20% of veterans reporting probable mild TBI (mTBI) [4].

Characterized by less than an 30 minutes loss of consciousness, post-traumatic amnesia under 24 hours and a Glasgow Coma Scale (GCS) score of 15-13 [5], mTBI is the most common (~85%) head trauma in both the military and civilian setting [6]. While most

Corresponding Author: Oded Gonen, PhD, Department of Radiology, New York University School of Medicine, 660 First Avenue, 4th Floor, New York, New York 10016, Telephone: (212) 263-3532, FAX: (212) 263-7541, oded.gonen@nyumc.org.

Conflicts of Interest: The authors declare that they have no conflict of interest.

patients experience full symptom resolution within months, 5 to 15% are diagnosed with persistent post-concussive syndrome (PPCS) to become what has been labeled the "Miserable Minority" [7].

TBI damage is assumed to result from the mechanical strain of sudden acceleration and deceleration that damages the axonal cytoskeleton and disrupts ionic balances. Abnormally high calcium influx impairs transport along the axon and can lead to dysfunction or axotomy followed by cell death [8, 9]. This strain can also cause vascular damage, seen by clinical MRI and CT, and crucial for the acute assessment of mTBI: Hemorrhages, hemosiderin and enlarged Virchow-Robin spaces [10]. All of these are presumed to be associated with underlying diffuse axonal injury (DAI) [11] which, however, is usually MRI and CT occult. This inability to assess the total disease load leads to weak correlation of imaging with clinical metrics [12], and motivates the search for other mTBI biomarkers to direct pharmacological regimens and predict outcome.

MRI occult mTBI damage can be studied with quantitative MR methods, *e.g.,* diffusion tensor [13], functional MRI [14], and proton MR spectroscopy (^{1}H-MRS) [15]. ^{1}H-MRS adds unique specificity to pathological processes by quantifying surrogates: *N*-acetylaspartate (NAA) for neuronal integrity, creatine (Cr) for cellular energy/density, choline (Cho) for membrane turnover and *myo*-inositol (*m*I) for astroglial proliferation [15]. Most studies, however, use single-voxel or 2D ^{1}H-MRS covering under 10% of the brain: regions-of-interest (ROIs) that may not be globally representative and that also make it impossible to distinguish focal from diffuse injury. In addition, quantification with metabolite ratios may confound interpretation since Cr (a frequent denominator) levels can also be abnormal [16, 17].

These shortcomings can be reduced with absolute metabolic quantification in multi-voxel ^{1}H-MR spectroscopic imaging (^{1}H-MRSI) over a much larger brain volume [18, 19]. Analyzing all voxels together improves the signal-to-noise ratio (SNR) for better precision, *i.e.* sensitivity to smaller global changes [20], at the cost of averaging out regional metabolic variations - a reasonable tradeoff for diffuse disorders. Since mTBI often leads to neurological symptoms even without clinical MRI findings, our goal was to test if DAI is quantifiable with ^{1}H-MRSI.

Materials and Methods

Human Subjects

Twenty-six closed head mTBI patients (5 women, 21 men), age 33±11 (mean ± standard deviation), age range 18 – 56 years, were recruited serially. Twenty-five were enrolled following emergency room visits with GCS score of 15-13 and confirmed loss of consciousness (LOC) of 30 minutes or less. Patient #13 was referred from a physician's office where mTBI diagnosis was based on clinical evaluation and 30 minutes LOC. Exclusion criteria were any MRI contraindications, substance dependencies, inability to give informed consent, HIV infection, prior TBI and history of any neurological disease. Patients' demographics are compiled in Table 1. Thirteen age- and gender-matched healthy controls (5 women, 8 men), age 33±12, age range 19 – 57,) year olds were enrolled. Their exclusion criteria were the same as the patients', plus any findings on their T1- and T2-weighted MRI. The study was approved by the institutional ethics committee and was in accordance with the ethical standards of the 1964 Declaration of Helsinki and all participants gave written informed consent.

MR Data Acquisition

All experiments were done in a 3 T MRI scanner (Trio, Siemens AG, Erlangen Germany) with a TEM3000 (MR Instruments, Minneapolis, MN) circularly-polarized transmit-receive head coil. For image-guidance of the ^{1}H-MRSI volume-of-interest (VOI), we acquired thirty 3.7 mm thick axial T2-weighted Fluid Attenuated Inversion Recovery (FLAIR) images: *TE/TI/TR*= 88/2500/9000 ms 256×256 mm^2 field-of-view (FOV) and 512×512 matrix. For tissue segmentation, sagittal Magnetization Prepared RApid Gradient Echo (MP-RAGE): *TE/TI/TR*= 2.6/800/1360 ms, was obtained at a FOV of 256×256×160 mm^3 and 256×256×160 matrix. They were reconstructed in axial, sagittal and coronal slices (1 mm^3 isotropic pixels) at an angle rendering the genu and splenium of the corpus callosum in the same horizontal plane at the level of the longitudinal fissure, as shown in Fig. 1a.

Our chemical-shift imaging (CSI) based auto-shim procedure then adjusted the scanner's first and second order currents in 3 – 5 minutes [21]. Next, a 10 cm anterior-posterior (AP) ×8 cm left-right (LR) ×4.5 cm inferior-superior (IS) = 360 cm^3 ^{1}H-MRSI VOI was image-guided over the corpus callosum, as shown in Fig. 1a-c. The VOI was excited with *TE/TR*=35/1800 ms PRESS in three 1.5 cm thick, second-order Hadamard encoded slabs (6 slices) interleaved every *TR* along the IS direction (see Fig. 1c) for optimal signal-to-noise ratio (SNR) and spatial coverage [22]. These slices were partitioned with 2D 16×16 CSI over a 16×16 cm^2 FOV, to yield 1.0×1.0×0.75 cm^3 nominal voxels, as shown in Fig. 1. The 8×10 cm (LR×AP) VOI was defined in their planes with two 11.2 ms long numerically optimized 180° RF pulses (4.5 kHz bandwidths) under 1.34 and 1.1 mT/m gradients to yield 8×10×6=480 voxels. The MR signal was acquired for 256 ms at ±1 kHz bandwidth. At two averages, the ^{1}H-MRSI took 34 minutes and the entire protocol was under an hour.

Voxel tissue Segmentation

The MP-RAGE images were segmented using SPM2 (Wellcome Department of Cognitive Neurology, Institute of Neurology, Queen Square, London, UK [23]) to obtain cerebrospinal fluid, white and gray matter (CSF, WM, GM) masks. These were co-registered with the ^{1}H-MRSI grid using in-house software (MATLAB 2009b, The Mathworks Inc., Natick, MA), as shown in Fig. 2, that yielded their volume contribution to every *j*-th voxel in the *k*-th subject: V_{jk}^{GM}, V_{jk}^{WM}, V_{jk}^{CSF}.

Metabolic quantification

The ^{1}H-MRSI data was processed offline using in-house software written in IDL (Research Systems Inc. Boulder CO). The data was voxel-shifted to align the NAA grid with the VOI. The data was then Fourier transformed in the time, AP and LR dimensions and Hadamard reconstructed along the IS direction. The 480 spectra were each frequency-aligned and zero-order phase corrected in reference to the NAA peak. Voxels which demonstrated lipid contamination were excluded from the analysis.

Relative levels of the *i*-th (*i*=NAA, Cr, Cho, *m*I) metabolite in the *j*-th (*j*=1…480) voxel in the k^{th} (*k*=1..39) subject were obtained from their peak area, S_{ijk}, using SITools-FITT parametric spectral modeling software package [24]. The S_{ijk}-s were scaled into absolute millimole amounts, Q_{ijk}, relative to a 2 L sphere of C_i^{vitro}=12.5, 10.0, 3.0 and 7.5 mM NAA, Cr, Cho and *m*I in water:

$$Q_{\text{ijk}}=\frac{C_i^{\text{vitro}}}{V}\cdot\frac{S_{\text{ijk}}}{S_{\text{ijR}}}\cdot\left(\frac{P_j^{180^\circ}}{P_R^{180^\circ}}\right)^{1/2}\ \text{millimoles}, \quad (1)$$

where V is the voxel volume, the S_{ijR} is the sphere's voxels' metabolites' signal, $P_j^{180°}$ and $P_R^{180°}$ the RF power for a non-selective 1 ms 180° inversion pulse on the k-th subject and reference.

Average VOI tissue concentrations, Q_{ik}, were corrected for the relaxation times differences between each metabolite, i, *in vivo* (T_1^{vivo}, T_2^{vivo}) and in the phantom (T_1^{vitro}, T_2^{vitro}), with:

$$f_i = \frac{\exp\left(-\mathrm{TE}/T_2^{\mathrm{vitro}}\right)}{\exp\left(-\mathrm{TE}/T_2^{\mathrm{vivo}}\right)} \cdot \frac{1-\exp\left(-\mathrm{TR}/T_1^{\mathrm{vitro}}\right)}{1-\exp\left(-\mathrm{TR}/T_1^{\mathrm{vivo}}\right)}. \quad (2)$$

Literature 3 T T_1^{vivo} [25] and T_2^{vitro}s [26, 27] were used. If values for GM and WM were reported separately, a weighted average of 3:2 WM:GM (the composition of the VOI) was calculated. For NAA, Cr, Cho and *m*I T_1^{vivo}s were 1360, 1300, 1145, 1170 ms and T_2^{vivo}s were 350, 174, 251, 200 ms. The corresponding values measured in the phantom were T_2^{vitro} = 483, 288, 200, 233 ms and T_1^{vitro} =605, 336, 235, 280 ms.

The average tissue concentration in the VOI for each metabolite, C_{ik} was obtained as:

$$C_{\mathrm{ik}} = \frac{\sum_{j=1}^{480} Q_{\mathrm{ijk}}}{\sum_{j=1}^{480}\left(V_{\mathrm{jk}}^{\mathrm{GM}} + V_{\mathrm{jk}}^{\mathrm{WM}}\right)} \cdot f_i \mathrm{mM}/g\mathrm{wetweight}. \quad (3)$$

The sum of all voxels, C_{ik} has the advantage of (number of voxels)^{½} ≈22 fold lower variance than individual voxels, and consequently is expected to yield better precision [20].

Global WM and GM concentrations

Since the CSF does not contribute to the ^{1}H-MRSI signals, the i-th metabolite amount in the j-th voxel in the k-th subject can be modeled as a sum of two compartments (GM, WM):

$$Q_{\mathrm{ijk}} = Q_{\mathrm{ijk}}^{\mathrm{GM}} + Q_{\mathrm{ijk}}^{\mathrm{WM}} = C_{\mathrm{ik}}^{\mathrm{GM}} \cdot V_{\mathrm{jk}}^{\mathrm{GM}} \cdot f_i^{\mathrm{GM}} + C_{\mathrm{ik}}^{\mathrm{WM}} \cdot V_{\mathrm{jk}}^{\mathrm{WM}} \cdot f_i^{\mathrm{WM}}, \quad (4)$$

where C_{ik}^{WM}, C_{ik}^{GM} are the k-th subject i-th metabolite (unknown) global WM and GM concentrations and f_i^{GM}, f_i^{WM} are given by Eq. (2) with T_2^{vivo}s of 275, 157, 241 and 200 ms for NAA, Cr, Cho and *m*I in GM; and 400, 185, 258 and 200 ms in WM [26, 27]. The GM and WM T_1^{vivo}, T_2^{vitro}s and T_1^{vitro}s, are the same as for Eq. (2), above.

Although C_{ik}^{WM} and C_{ik}^{GM} cannot both be derived from Eq. (4), since the brain's GM and WM heterogeneity is on a scale smaller than the 1 cm^3 ^{1}H-MRSI voxels, each voxel will have different V_{jk}^{WM} and V_{jk}^{GM} independent coefficients. The resulting over-determined 480 equation system, was therefore, solved for the optimal C_{ik}^{WM} and C_{ik}^{GM} using linear regression [19].

Statistical Analyses

Two-way analysis of variance (ANOVA) was used to compare patients' with controls' mean of each metabolite. A separate analysis was conducted for each metabolite, globally, in WM and GM. In each case, the observed metabolite values constituted the dependent variable, while the model included subject group as a classification factor and the error variance was allowed to differ across subject groups to remove the unnecessary assumption of variance homogeneity. Since controls were matched to patients in age and gender, the indicator

variable identifying subjects that were matched was included in the model as a blocking factor. As a result, the comparisons of global and tissue specific concentrations were adjusted for age and gender. Reported *p* values are two-sided, defined as significant for $p<0.05$, except for the NAA. Since it is known to always be lower in all adult neuropathologies we looked for single-sided *p*-values. Pearson and Spearman correlations were used to look for relationships between concentrations and time from injury. SAS 9.0 (SAS Institute, Cary, NC) was used for all computations.

Results

The patients GCS was 14.7±0.5 (mean ± standard deviation) and their mean time from injury was 21 days (range: 3 - 55 days), as shown in Table 1. Of the four mTBI patients who had positive MRI findings, only two #11 and #16′s may have been directly related to their head trauma. Five patients were on medications for a trauma-induced symptom.

Our automatic shim yielded consistent 26±3 Hz whole-head FWHM water line that decreased to 21±3 Hz in the VOI without additional adjustments. An example of VOI size, position and spectra, is shown in Fig. 1. Occasional lipid contamination caused between zero to at most ten voxels per dataset to be excluded from the analysis. The metabolites' SNRs in the remaining ~18,720 voxels (39 subjects ×480 voxels each) were: NAA=30±7, Cr=15±3, Cho=13±3 and *m*I=8±1 and the average linewidth was 6.6±2.0 Hz. Under 1% of the voxels contained >90% GM and 20% had WM fractions >90%, *i.e.* could be considered “pure.”

The spectra summed from all the 480 VOI voxels (equivalent to the numerator of Eq. (3)) from every subject, overlaid with their fits, are shown in Fig. 3. They exhibit NAA, Cr, Cho and *m*I SNRs of: 561±74, 265±34, 228±32 and 128±17, a dramatic $\sim 480^{1/2} \approx 22$ gain over the original 0.75 cm^3 voxels (compare Fig. 3 with Fig. 1d) and linewidths of 6.5±0.6 Hz, retaining the single-voxel spectral resolution [18].

The metabolites' whole VOI concentrations (Eq. (3)) as well as its WM and GM moieties (Eq. (4)) are given in Table 2 and their distributions plotted in Fig. 4. Patients' Cr, Cho and *m*I concentrations were not different from the controls' either in the VOI, its WM or GM. The NAA concentrations, however, were significantly lower in patients' VOI (7.4±0.6 versus 7.9±0.6 mM, $p=0.0180$) and in their WM (7.2±0.8 versus 7.7±0.6 mM, $p=0.0125$) but *not* GM, as shown in Fig. 4. While the VOI NAA deficit reduced to a trend upon application of Bonferroni correction for multiple comparisons, the WM change remained significant. To account for disease duration we looked for association between all concentrations and time from injury, and found significant Pearson and Spearman correlations in WM Cho (0.004 mM/day, r=0.4, $p=0.043$ and r=0.43 $p=0.028$) and Pearson correlation WM Cr (0.013 mM/day, r=0.39, $p=0.049$), as shown in Fig. 5.

Discussion

^{1}H-MRS Sensitivity to mTBI

The advantages of ^{1}H-MRS over other quantitative MR techniques are specificity to injury type through metabolites indicative of different processes, sensitivity to non-structural injury and to GM status. Since the first ^{1}H-MRS study of mTBI implicated the splenium of the corpus callosum [28] abnormalities have been reported in the parietal, temporal, occipital [29, 30] and frontal [30-33] lobes, peri-contusional [34, 35], as well as supraventricular areas [16, 17]. However, when the same regions are examined, some cohorts show abnormalities [17, 31] while others do not [29].

Direct comparisons of mTBI findings is difficult, however, due to different time from TBI, injury heterogeneity, use of single-voxel ^{1}H-MRS and of metabolic ratios that assume stable Cr concentration. For example, lower NAA/Cr usually attributed to NAA reduction is confounded by evidence of increased Cr [16, 17]. Indeed, the pioneering report of Cecil *et al.* [28] had attributed lower NAA/Cr in the splenium to NAA deficit, whereas absolute quantification in that structure revealed normal NAA and increased Cr [16]. Yet, only four mTBI ^{1}H-MRS studies used absolute quantification [16, 17, 30, 36], and just one in substantial volume [30]. Although it also reported WM reduced NAA, it included moderate TBI, hence, it is not directly comparable to our study.

Two main points can be surmised from past research: *(i)* mTBI is likely a diffuse/multi-focal condition with no specific region(s) consistently involved. Subjectively chosen ROIs, therefore, may miss some patients' pathology, reducing statistical power and underscoring the need for extensive volume coverage. *(ii)* Higher ^{1}H-MRS sensitivity is needed: *e.g.* of the 25 ROIs in one study almost 70% had consistent *trends* for abnormalities, without statistical significance [29]. Single voxels, however, are unable to differentiate focal from diffuse disease and must balance SNR, spatial resolution (partial volume) and coverage. Specifically, small ROIs may lack sensitivity and bigger ones suffer GM/WM/CSF partial volume that can vary their metabolites' levels to confound injury related changes (see cautionary note below).

To address both sensitivity and limited coverage and to test the hypothesis that mTBI results in diffuse sequelae, we used a large (360 cm^3) VOI, in which every voxel's spectrum contributed to calculating each metabolite's concentration [18, 19]. Analyzing many (480) voxels simultaneously increased the precision, reflected by ~10% coefficients of variation in the controls, as good or better than other ^{1}H-MRS methods. Importantly, any abnormalities detected this way must be diffuse since focal changes would be averaged out.

Diffuse abnormalities

It is well documented that TBI involves diffuse changes that may determine adverse outcomes [37, 38]. While hemorrhages are markers for DAI on conventional imaging, most mTBI patients have unremarkable MRI/CT [11] and are rarely available for *post-mortem* study. Consequently, hypotheses on their pathologies are mostly based on histology of more severe TBI and animal models that lack the heterogeneity of human injury [38]. Fortunately, indirect evidence of mTBI changes has been obtained by quantitative MR methods, *e.g.*, DTI [13], functional MRI [14] and ^{1}H-MRS [15]. If the injury loci are different among patients [39], however, ROI-based studies cannot differentiate focal from diffuse injury. Our results support the DAI hypothesis in mTBI.

Axonal pathology

Axons are known to be vulnerable to the inertial forces of blunt head trauma. A large body of evidence from *ex vivo* animal and human TBI studies suggests that the initial site of injury is the axolemma via disruption of ionic channels [38, 39]. Calcium influx impairs axonal transport, resulting in axonal swelling and potential axotomy [8, 9] that may be followed by Wallerian and retrograde degeneration and ultimately cell necrosis or apoptosis [9].

The observed NAA decrease in the WM cannot distinguish cell death from dysfunction. The latter, however, is supported by the lack of difference in patients' Cr, Cho and *m*I levels from controls'. Normal Cho in patients may indicate *absence* of fragmented myelin from axons swelling or degenerating, as also suggested by DTI data [40]. Furthermore, normal *m*I and Cr that originate from intracellular stores in astrocytes [41] may represent lack of

astroglial hypertrophy or hyperplasia from the astroglial scarring that typically forms on severed axons associated with permanent neuronal injury in more severe TBI [42]. In addition, normal GM NAA here and in other mTBI studies [16, 17] suggests no cell body injury from Wallerian degeneration. This process in humans, however, is thought to take several months [8] and it can be conjectured, therefore, that the correlations of Cho and Cr with time in our cohort may represent its progression. Given their cross-sectional nature, however, these correlations need to be interpreted with caution until verified by a longitudinal study.

While it is unclear whether cell death is characteristic of early mTBI, even if it occurs, it is unlikely to be widespread [9, 39]. Rather, axons may convert to a dysfunctional state from which they may recover [9], as evidenced by NAA levels in serial ^{1}H-MRS studies [32, 33, 43]. Our data supports the current consensus that brain injury is on a continuum [11, 39, 40], *i.e.* DAI occurs in mTBI to a lesser degree compared to more severe trauma. In addition, if axonal dysfunction and not death dominates mTBI pathology, it is important to reiterate the danger of a second traumatic event [39], and underscore potential benefits of suitable therapy.

Finally, only two patients, 8%, had (potentially) injury-related MRI findings, which would qualify them as “complicated mTBI” [11]. This is much lower than the 17% rate of CT findings reported by Stein *et al.* in 1538 patients [44], and may reflect the fact that 80% of our patients had GCS of 15, that is associated with a 5% findings rate [45]. Since it is well known that severity differs across the ‘mild’ range, *i.e.* not all GCS in mTBI are equivalent [46], it is noteworthy that our patient population suffered relatively milder (more subtle) injury than the common mTBI. Our results, therefore, suggest the presence of DAI in patients with mostly normal GCS scores and MRI scans, *i.e.* injury missed by the clinical and radiological exams.

A cautionary note

Even at relatively high (0.75 cm^3) spatial resolution only 20% of the VOI voxels contained 90% or more WM (considered “pure”) and under 1% were over 90% GM. The different GM and WM metabolites' concentrations present a confounding scenario: different voxel placement (in a serial or cross-sectional study) can alter its WM/GM fractions, hence, ^{1}H-MRS signal, regardless of any underlying pathology. Since early changes in mTBI are small, placing a voxel in a WM region with unaccounted for GM partial volume will boost its NAA signal (that is ~15% higher in GM) sufficiently to offset its ~7% pathology driven deficit, or introduce enough variations to render differences insignificant. This underscores the importance of tissue segmentation and that attempts to place voxels in “pure” WM or GM to circumvent this need are unlikely to be reliable.

Caveats

This study is also subject to some limitations. First, since it is geared to maximize sensitivity at the expense of localization (although the original 3D data remains available), it is insensitive to focal changes that may occur only in specific small brain region(s). For example, while Cr levels were normal in the global WM, this may not necessarily be the case locally [16, 17]. For our approach to yield significant differences, however, changes must be present in a substantial part of our VOI. What is demonstrated here, therefore, is not the absence of local injury, but rather the presence of a diffuse component. Second, while we demonstrate that this diffuse injury is axonal, its correspondence to histopathologically defined DAI [8, 47] remains unclear. Also known as “traumatic axonal injury”, DAI is characterized by the presence of axonal swellings which can only be conclusively diagnosed *post-mortem* [47]. Structurally intact axons can also be affected [47], however, and diffusely

lower NAA levels can represent manifestations of both types of DAI sequelae with an unknown contribution of each. Third, is the assumption that GM and WM metabolites' concentrations do not vary much over the VOI. While concentrations *between* tissue types differ significantly, *within*-tissue variations are small and in the forebrain exist only for NAA and Cho (mostly between the thalamus and cortical GM) [48]. Even then, if these differences are the same for all subjects, the only constraint would be that the changes be uniform (all increases or all decreases), a reasonable assumption given the NAA decreases, Cr, Cho and *m*I increases reported in TBI [15]. Fourth, although our VOI covered substantially more brain than most previous studies, it excluded most of the cortex (it contained ~40% of the brain's ~470 cm^3 WM volume [49], as well as cortical GM and all deep GM structures). Finally, acquisition and post-processing duration may limit the clinical application of the technique in its current form.

Conclusion

We report evidence of DAI in recent "non-complicated" mTBI patients assessed by global quantitative ^{1}H-MRS. The lack of glial WM abnormalities and any GM injury within two months from mTBI suggests white matter dysfunction rather than degeneration and underscores the potential for axonal recovery.

Acknowledgments

This work was supported by National Institutes of Health Grants EB01015, NS39135, NS29029 and NS050520. Assaf Tal is also supported by the Human Frontiers Science Project. We thank Ms. Nissa Perry and Mr. Joseph Reaume for subject recruitment.

References

1. Faul, M.; Xu, L.; Wald, M.; Coronado, V. Traumatic Brain Injury in the United States: Emergency Department Visits, Hospitalizations and Deaths, 2002-2006. Centers for Disease Control and Prevention, National Center for Injury Prevention and Control; Atlanta GA: 2010.
2. Zaloshnja E, Miller T, Langlois JA, Selassie AW. Prevalence of long-term disability from traumatic brain injury in the civilian population of the United States, 2005. J Head Trauma Rehabil. 2008; 23:394–400. [PubMed: 19033832]
3. Snell FI, Halter MJ. A signature wound of war: mild traumatic brain injury. J Psychosoc Nurs Ment Health Serv. 2010; 48:22–28. [PubMed: 20166653]
4. Tanelian, T.; Jaycox, LH. Report. RAND Corporation; Santa Monica, CA: 2008. Invisible wounds of war; p. 305
5. Teasdale G, Jennett B. Assessment of coma and impaired consciousness. A practical scale. Lancet. 1974; 2:81–84. [PubMed: 4136544]
6. MacGregor AJ, Shaffer RA, Dougherty AL, Galarneau MR, Raman R, Baker DG, Lindsay SP, Golomb BA, Corson KS. Prevalence and psychological correlates of traumatic brain injury in operation iraqi freedom. J Head Trauma Rehabil. 2010; 25:1–8. [PubMed: 20051901]
7. Ruff R. Two decades of advances in understanding of mild traumatic brain injury. J Head Trauma Rehabil. 2005; 20:5–18. [PubMed: 15668567]
8. Buki A, Povlishock JT. All roads lead to disconnection?--Traumatic axonal injury revisited. Acta Neurochir (Wien). 2006; 148:181–193. discussion 193-184. [PubMed: 16362181]
9. Iverson GL. Outcome from mild traumatic brain injury. Curr Opin Psychiatry. 2005; 18:301–317. [PubMed: 16639155]
10. Inglese M, Bomsztyk E, Gonen O, Mannon LJ, Grossman RI, Rusinek H. Dilated perivascular spaces: hallmarks of mild traumatic brain injury. AJNR Am J Neuroradiol. 2005; 26:719–724. [PubMed: 15814911]
11. Bigler ED. Neuroimaging in Mild Traumatic Brain Injury. Psychological Injury and Law. 2010

12. Wilson JT, Wiedmann KD, Hadley DM, Condon B, Teasdale G, Brooks DN. Early and late magnetic resonance imaging and neuropsychological outcome after head injury. J Neurol Neurosurg Psychiatry. 1988; 51:391–396. [PubMed: 3361330]
13. Niogi SN, Mukherjee P. Diffusion tensor imaging of mild traumatic brain injury. J Head Trauma Rehabil. 2010; 25:241–255. [PubMed: 20611043]
14. Mayer AR, Mannell MV, Ling J, Gasparovic C, Yeo RA. Functional connectivity in mild traumatic brain injury. Hum Brain Mapp. 2011
15. Marino S, Ciurleo R, Bramanti P, Federico A, De Stefano N. 1H-MR spectroscopy in traumatic brain injury. Neurocrit Care. 2010; 14:127–133. [PubMed: 20737247]
16. Gasparovic C, Yeo R, Mannell M, Ling J, Elgie R, Phillips J, Doezema D, Mayer A. Neurometabolite Concentrations in Gray and White Matter in Mild Traumatic Brain Injury: A 1HMagnetic Resonance Spectroscopy Study. J Neurotrauma. 2009
17. Yeo RA, Gasparovic C, Merideth F, Ruhl D, Doezema D, Mayer AR. A longitudinal proton magnetic resonance spectroscopy study of mild traumatic brain injury. J Neurotrauma. 2011; 28:1–11. [PubMed: 21054143]
18. Kirov II, George IC, Jayawickrama N, Babb JS, Perry NN, Gonen O. Longitudinal inter- and intra-individual human brain metabolic quantification over 3 years with proton MR spectroscopy at 3 T. Magn Reson Med. 2012; 67:27–33. [PubMed: 21656555]
19. Tal A, Kirov I, Grossman RI, Gonen O. The Role of Gray and White Matter Segmentation in Quantitative Proton MR Spectroscopic Imaging. NMR in Biomedicine. 2012 In Press.
20. Kreis R, Slotboom J, Hofmann L, Boesch C. Integrated data acquisition and processing to determine metabolite contents, relaxation times, and macromolecule baseline in single examinations of individual subjects. Magn Reson Med. 2005; 54:761–768. [PubMed: 16161114]
21. Hu J, Javaid T, Arias-Mendoza F, Liu Z, McNamara R, Brown TR. A fast, reliable, automatic shimming procedure using 1H chemical-shift-imaging spectroscopy. J Magn Reson B. 1995; 108:213–219. [PubMed: 7670755]
22. Goelman G, Liu S, Hess D, Gonen O. Optimizing the efficiency of high-field multivoxel spectroscopic imaging by multiplexing in space and time. Magn Reson Med. 2006; 56:34–40. [PubMed: 16767711]
23. Ashburner J, Friston K. Multimodal image coregistration and partitioning--a unified framework. Neuroimage. 1997; 6:209–217. [PubMed: 9344825]
24. Soher BJ, Young K, Govindaraju V, Maudsley AA. Automated spectral analysis III: application to in vivo proton MR spectroscopy and spectroscopic imaging. Magn Reson Med. 1998; 40:822–831. [PubMed: 9840826]
25. Traber F, Block W, Lamerichs R, Gieseke J, Schild HH. 1H metabolite relaxation times at 3.0 tesla: Measurements of T1 and T2 values in normal brain and determination of regional differences in transverse relaxation. J Magn Reson Imaging. 2004; 19:537–545. [PubMed: 15112302]
26. Kirov I, Fleysher L, Fleysher R, Patil V, Liu S, Gonen O. Age dependence of regional proton metabolites T2 relaxation times in the human brain at 3 T. Magn Reson Med. 2008; 60:790–795. [PubMed: 18816831]
27. Posse S, Otazo R, Caprihan A, Bustillo J, Chen H, Henry PG, Marjanska M, Gasparovic C, Zuo C, Magnotta V, Mueller B, Mullins P, Renshaw P, Ugurbil K, Lim KO, Alger JR. Proton echo-planar spectroscopic imaging of J-coupled resonances in human brain at 3 and 4 Tesla. Magn Reson Med. 2007
28. Cecil KM, Hills EC, Sandel ME, Smith DH, McIntosh TK, Mannon LJ, Sinson GP, Bagley LJ, Grossman RI, Lenkinski RE. Proton magnetic resonance spectroscopy for detection of axonal injury in the splenium of the corpus callosum of brain-injured patients. J Neurosurg. 1998; 88:795–801. [PubMed: 9576245]
29. Govindaraju V, Gauger GE, Manley GT, Ebel A, Meeker M, Maudsley AA. Volumetric proton spectroscopic imaging of mild traumatic brain injury. AJNR Am J Neuroradiol. 2004; 25:730–737. [PubMed: 15140711]
30. Govind V, Gold S, Kaliannan K, Saigal G, Falcone S, Arheart KL, Harris L, Jagid J, Maudsley AA. Whole-brain proton MR spectroscopic imaging of mild-to-moderate traumatic brain injury

and correlation with neuropsychological deficits. J Neurotrauma. 2010; 27:483–496. [PubMed: 20201668]

31. Garnett MR, Blamire AM, Rajagopalan B, Styles P, Cadoux-Hudson TA. Evidence for cellular damage in normal-appearing white matter correlates with injury severity in patients following traumatic brain injury: A magnetic resonance spectroscopy study. Brain. 2000; 123:1403–1409. [PubMed: 10869052]
32. Vagnozzi R, Signoretti S, Tavazzi B, Floris R, Ludovici A, Marziali S, Tarascio G, Amorini AM, Di Pietro V, Delfini R, Lazzarino G. Temporal window of metabolic brain vulnerability to concussion: a pilot 1H-magnetic resonance spectroscopic study in concussed athletes--part III. Neurosurgery. 2008; 62:1286–1295. discussion 1295-1286. [PubMed: 18824995]
33. Vagnozzi R, Signoretti S, Cristofori L, Alessandrini F, Floris R, Isgro E, Ria A, Marziale S, Zoccatelli G, Tavazzi B, Del Bolgia F, Sorge R, Broglio SP, McIntosh TK, Lazzarino G. Assessment of metabolic brain damage and recovery following mild traumatic brain injury: a multicentre, proton magnetic resonance spectroscopic study in concussed patients. Brain. 2010; 133:3232–3242. [PubMed: 20736189]
34. Son BC, Park CK, Choi BG, Kim EN, Choe BY, Lee KS, Kim MC, Kang JK. Metabolic changes in pericontusional oedematous areas in mild head injury evaluated by 1H MRS. Acta Neurochir Suppl. 2000; 76:13–16. [PubMed: 11449991]
35. Nakabayashi M, Suzaki S, Tomita H. Neural injury and recovery near cortical contusions: a clinical magnetic resonance spectroscopy study. J Neurosurg. 2007; 106:370–377. [PubMed: 17367057]
36. Kirov I, Fleysher L, Babb JS, Silver JM, Grossman RI, Gonen O. Characterizing ‘mild’ in traumatic brain injury with proton MR spectroscopy in the thalamus: Initial findings. Brain Inj. 2007; 21:1147–1154. [PubMed: 17882630]
37. Farkas O, Povlishock JT. Cellular and subcellular change evoked by diffuse traumatic brain injury: a complex web of change extending far beyond focal damage. Prog Brain Res. 2007; 161:43–59. [PubMed: 17618969]
38. Graham DI, McIntosh TK, Maxwell WL, Nicoll JA. Recent advances in neurotrauma. J Neuropathol Exp Neurol. 2000; 59:641–651. [PubMed: 10952055]
39. Biasca N, Maxwell WL. Minor traumatic brain injury in sports: a review in order to prevent neurological sequelae. Prog Brain Res. 2007; 161:263–291. [PubMed: 17618984]
40. Kraus MF, Susmaras T, Caughlin BP, Walker CJ, Sweeney JA, Little DM. White matter integrity and cognition in chronic traumatic brain injury: a diffusion tensor imaging study. Brain. 2007; 130:2508–2519. [PubMed: 17872928]
41. Frahm, J.; Hanefeld, F. Localized proton magnetic spectroscopy of brain disorders in childhood. In: Bachelard, HS., editor. Magnetic Resonance Spectroscopy and Imaging in Neurochemistry. Plenum Press; New York: 1997. p. 329-402.
42. Di Giovanni S, Movsesyan V, Ahmed F, Cernak I, Schinelli S, Stoica B, Faden AI. Cell cycle inhibition provides neuroprotection and reduces glial proliferation and scar formation after traumatic brain injury. Proc Natl Acad Sci U S A. 2005; 102:8333–8338. [PubMed: 15923260]
43. Friedman SD, Brooks WM, Jung RE, Chiulli SJ, Sloan JH, Montoya BT, Hart BL, Yeo RA. Quantitative proton MRS predicts outcome after traumatic brain injury. Neurology. 1999; 52:1384–1391. [PubMed: 10227622]
44. Stein SC, Ross SE. Mild head injury: a plea for routine early CT scanning. J Trauma. 1992; 33:11–13. [PubMed: 1635094]
45. Borg J, Holm L, Cassidy JD, Peloso PM, Carroll LJ, von Holst H, Ericson K. Diagnostic procedures in mild traumatic brain injury: results of the WHO Collaborating Centre Task Force on Mild Traumatic Brain Injury. J Rehabil Med. 2004:61–75. [PubMed: 15083871]
46. Culotta VP, Sementilli ME, Gerold K, Watts CC. Clinicopathological heterogeneity in the classification of mild head injury. Neurosurgery. 1996; 38:245–250. [PubMed: 8869050]
47. Johnson VE, Stewart W, Smith DH. Axonal pathology in traumatic brain injury. Exp Neurol. 2012
48. Baker EH, Basso G, Barker PB, Smith MA, Bonekamp D, Horska A. Regional apparent metabolite concentrations in young adult brain measured by (1)H MR spectroscopy at 3 Tesla. J Magn Reson Imaging. 2008; 27:489–499. [PubMed: 18307197]

49. Ge Y, Grossman RI, Babb JS, Rabin ML, Mannon LJ, Kolson DL. Age-related total gray matter and white matter changes in normal adult brain. Part I: volumetric MR imaging analysis. AJNR Am J Neuroradiol. 2002; 23:1327–1333. [PubMed: 12223373]

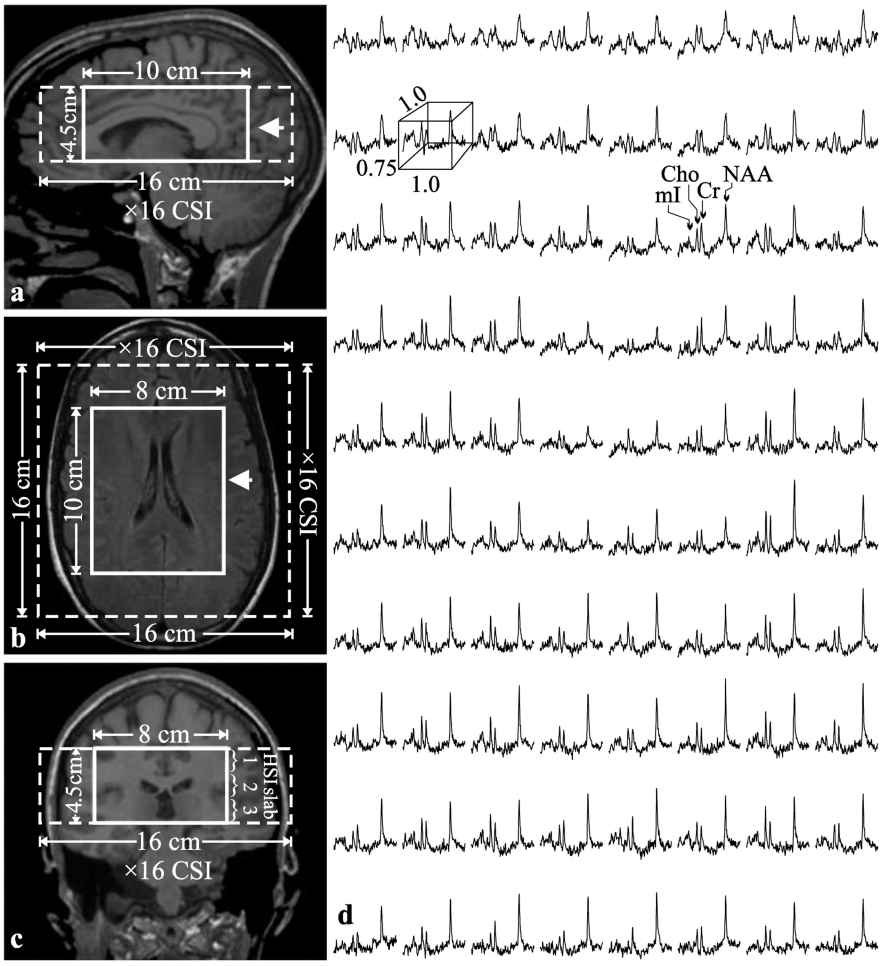

Fig. 1. Positioning of the ^{1}H-MRS VOI

Left: Sagittal (**a**) and coronal (**b**) T_1-weighted and axial T_2-weighted FLAIR MRI (**c**) of patient#18, superimposed with the 8×10×4.5 cm^3 VOI (LR×AP×IS - thick solid white line) and 16×16×4.5 cm^3 FOV (dashed white line). The arrow on each image indicates the spatial position of the image below. Right: (**d**) Real part of the 8×10 (LR×AP) ^{1}H spectra matrix from the VOI on the axial image. All spectra are on common frequency (1.3 to 3.9 ppm) and intensity scales. Note the SNR and spectral resolution obtained from these 1.0×1.0×0.75 cm^3 (LR×AP×IS) voxels in ~30 minutes of acquisition.

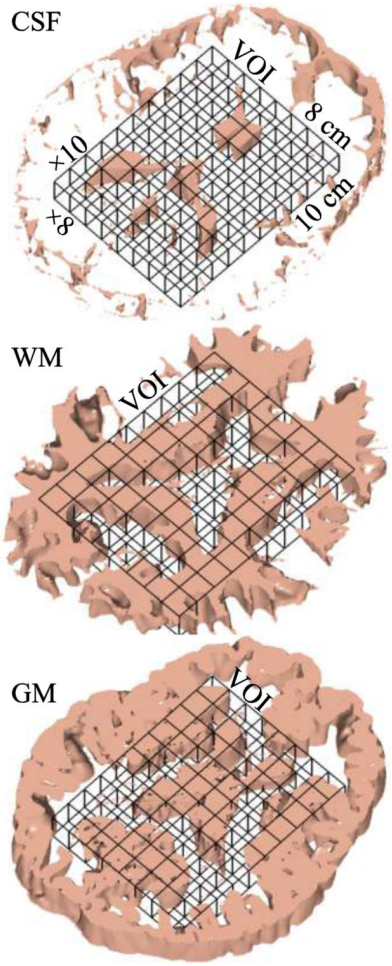

Fig. 2. ^{1}H-MRS - MRI co-registration

3D renderings of one of the six 7.5 mm thick spectroscopic slices in patient#12 in Table 1, co-registered with its 7.5 corresponding CSF, WM and GM masks (1 mm thick each) segmented from the T1-weighted MRI using SPM. Our in-house software counted how many pixels of each mask fell into every spectroscopic voxel in the VOI to estimate its volume for the analysis of Eqs. (3) and (4).

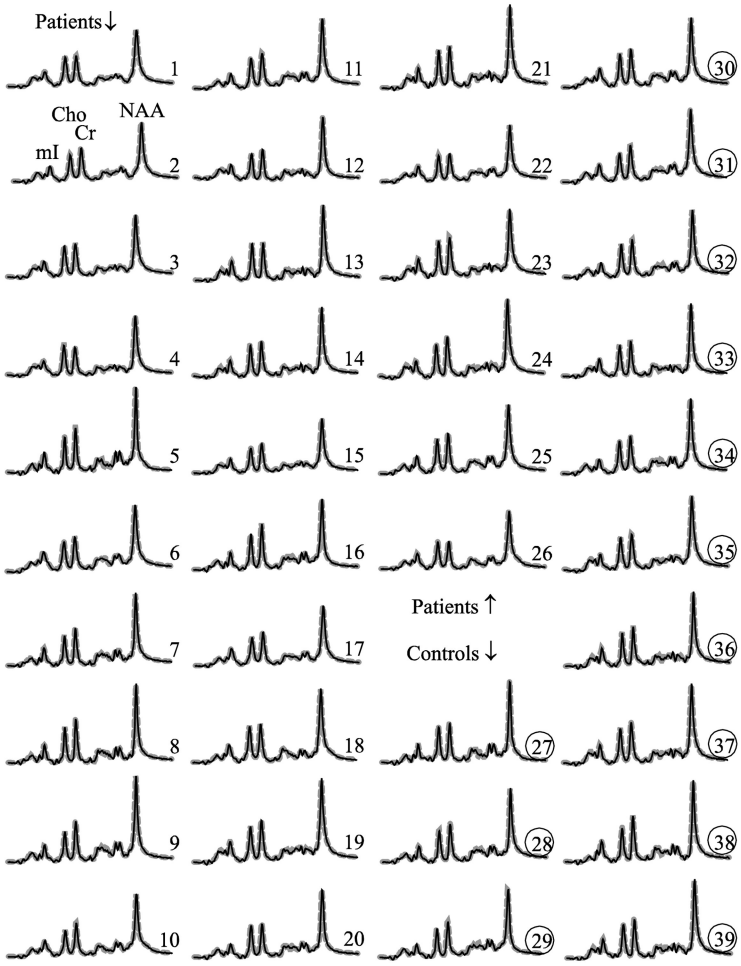

Fig. 3. Whole VOI ^{1}H-MRS spectra

Real part of the aligned and summed ^{1}H spectra from all the voxels in the VOI (thin black lines) representing Eq. (3), of each of the 26 patients (1–26) and 13 controls (27–39, circled), superimposed with the sum of the fitted model functions (thick dashed gray lines). All are on common intensity and chemical shift scales. Note the excellent SNRs and spectral resolution obtained, as well as the visual similarity in Cr, Cho and *m*I levels between patients and controls *versus* decreased NAA.

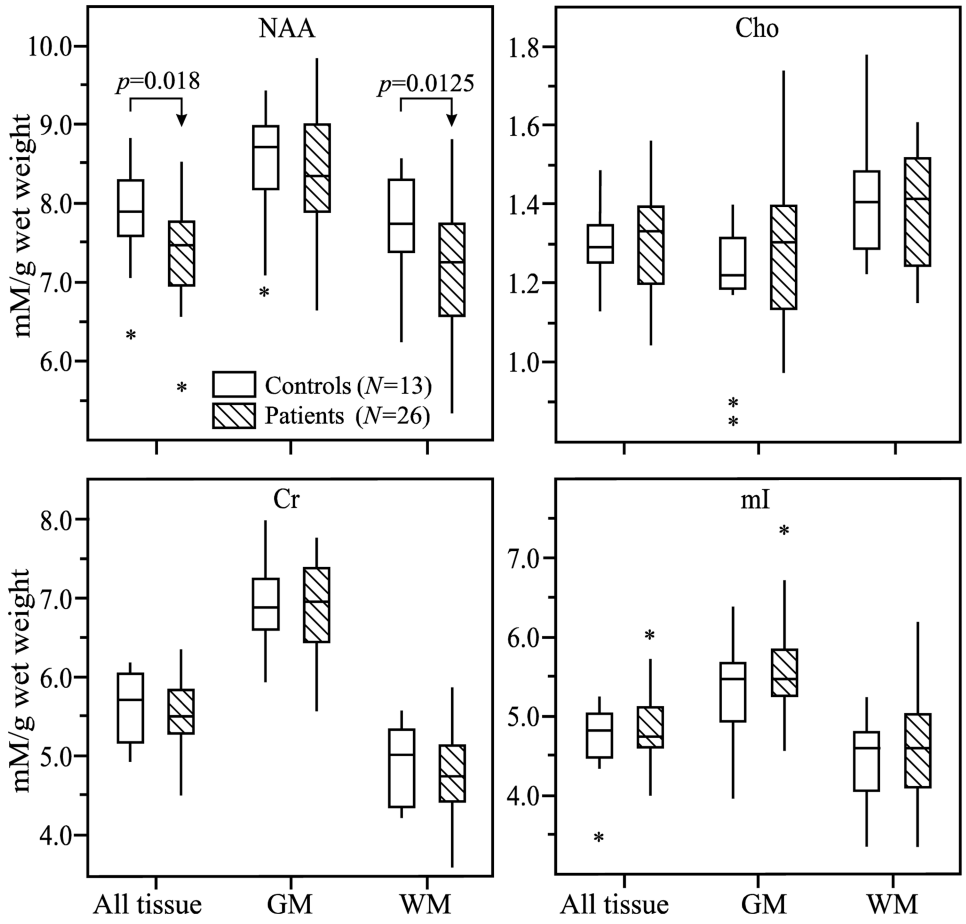

Fig. 4. Metabolic concentrations in GM and WM

Box plots displaying 25%, median and 75% (box), 95% (whiskers) and outliers (*) of the NAA, Cr, Cho and *m*I concentrations distributions in the VOI (all tissue) and its GM and WM compartments mTBI patients and controls. Note that the significant decrease (arrows) of NAA in the VOI that is entirely attributable to the WM pathology.

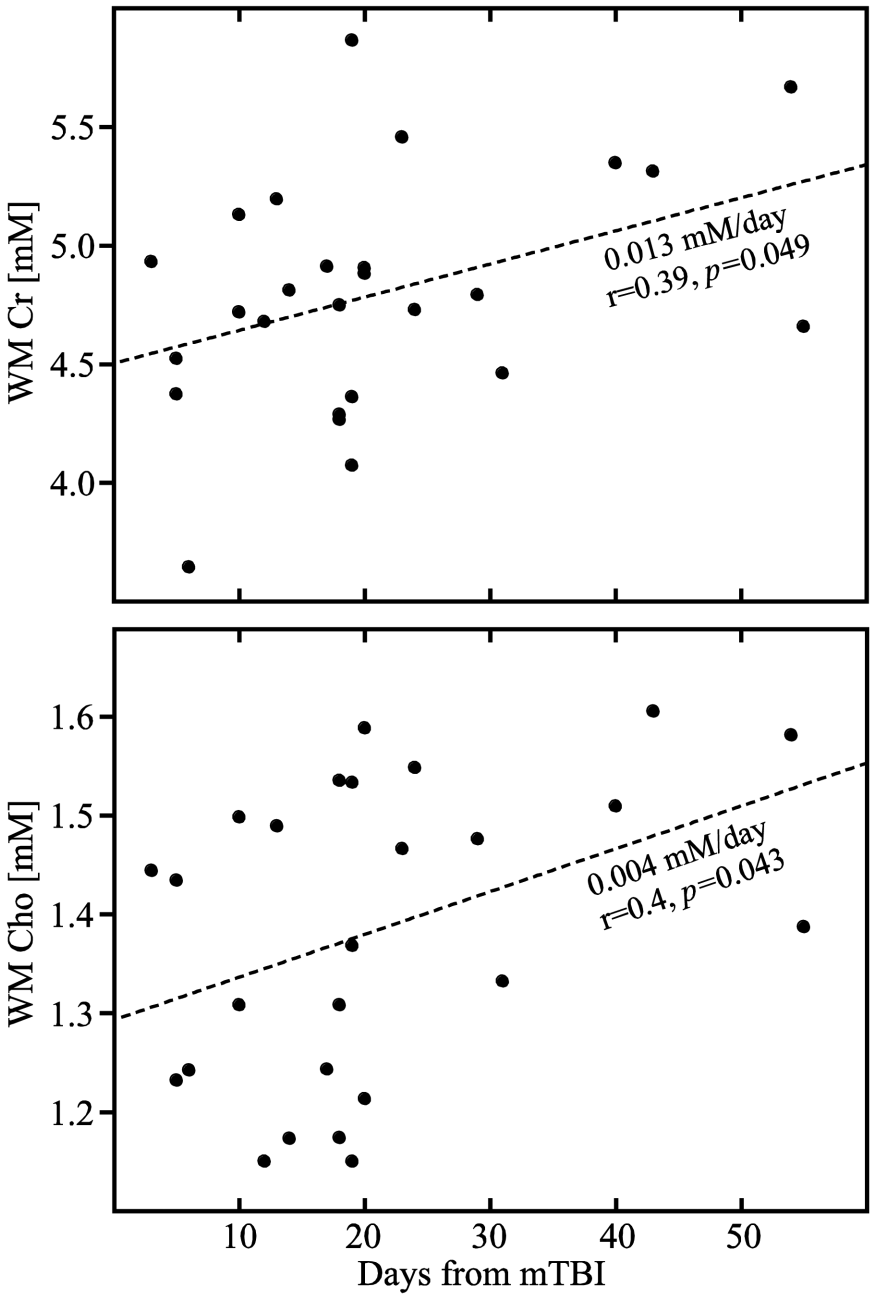

Fig. 5. White matter creatine and choline increase with time

Correlation plots of the patients' (●) white matter Cr (top) and Cho (bottom) concentrations versus their time from injury (in days). Note that the significant cross-sectional increase in both metabolites with time from injury is only in the WM (and not in GM) indicating possible evolving axonal pathology with sparing of the cell bodies.

Table 1

Patients (sorted by time from mTBI) demographics and imaging findings.

Patient	Age/Gender	TBI Cause	GCS	LOC duration[1]	Time from injury[2]	Self-reported symptoms on scan date[3]	MRI Findings
1	40/M	Fall	15	3	3	NS, V	Unremarkable
2	41/M	Fall	15	<1	5	NS, H, D, S	“
3	42/M	Fall	14	5	5	H, N, S, M	“
4	22/M	Assault	13	30	6	NS, H, N, P	“
5	18/M	Assault	15	20	10	None	“
6	25/M	Assault	15	25	10	H	Right frontal convexity arachnoid cyst
7	27/M	Assault	15	<1	12	None	Unremarkable
8	29/M	Bike fall	15	15	13	“	“
9	25/F	[4] Ped/Auto	15	2	14	“	“
10	32/M	Assault	15	2	17	H, D, S, M	“
11	23/M	Assault	14	30	18	None	Two ovoid foci of abnormal T2 hyperintensities in left frontal lobe subcortical white matter with nonspecific etiology
12	23/M	Assault	15	30	18	NS, H, D, N, M	Unremarkable
13	24/M	Assault	n/a	30	18	None	“
14	18/M	Ped/Auto	15	15	19	H, D, M	“
15	19/M	Assault	14	30	19	None	“
16	51/M	[5] MVA	14	30	19	NS, H	Few punctate foci of abnormal T2 hyperintensities in frontal and parietal lobe subcortical white matter with nonspecific etiology
17	37/M	Fall	15	2	20	NS, H, D, N, P	Unremarkable
18	51/F	Bike fall	14	30	20	NS, H, D, N, P, S, PH	Stable right cerebellopontine angle arachnoid cyst
19	36/M	Fall	15	<1	23	None	Unremarkable
20	35/M	Sport collision	15	<1	24	“	“
21	28/F	[6] Bike/Auto	15	20	29	NS, H, D, N, P, S	“
22	38/M	Fall	15	<1	31	None	“
23	56/M	Assault	15	<1	40	NS, P	“
24	32/F	Fall	15	1	43	NS, D, M	“
25	44/F	Ped/Auto	15	<1	54	D, P, M	“
26	50/M	Fall	15	<1	55	NS, H, D, N, P, S, M, PH	“

Patient	Age/Gender	TBI Cause	GCS	LOC duration[1]	Time from injury[2]	Self-reported symptoms on scan date[3]	MRI Findings
Avg.	**33±11**		**14.7±0.5**	**12±13**	**21±14**		

[1] Minutes,

[2] Days,

[3] most to least common: H - headache, NS - neck stiffness, D - dizziness, M -memory deficits, N - nausea, P - photophobia, S - sleep disturbance, PH - paresthesia (hand), V - blurred vision,

[4] Ped/Auto – pedestrian struck by car.

[5] MVA – motor vehicle accident.

[6] Bike/Auto – bicyclist struck by car. Bold: average ± standard deviation.

Table 2

Mean ± standard deviation of the metabolic concentrations inside the VOI: all-tissue (using Eq. (3)) and its WM and GM moieties (from Eq. (4)), within each subject group. Bold typeface indicates statistically significant difference ($p<0.05$).

		Concentration (mM/g wet-weight)			
		NAA	**Cr**	**Cho**	***m*I**
All tissue	Controls	**7.9±0.6**	5.6±0.5	1.3±0.1	4.7±0.5
	Patients	**7.4±0.6**	5.5±0.5	1.3±0.1	4.8±0.5
WM	Controls	**7.7±0.6**	4.9±0.5	1.4±0.1	4.4±0.6
	Patients	**7.2±0.8**	4.8±0.5	1.4±0.2	4.6±0.7
GM	Controls	8.5±0.7	6.9±0.6	1.2±0.2	5.3±0.6
	Patients	8.4±0.7	6.9±0.6	1.3±0.2	5.5±0.6